



## Electromechanical properties of $\text{Pb}(\text{In}_{1/2}\text{Nb}_{1/2})\text{O}_3\text{--Pb}(\text{Mg}_{1/3}\text{Nb}_{2/3})\text{O}_3\text{--PbTiO}_3$ single crystals

Fei Li, Shujun Zhang, Dabin Lin, Jun Luo, Zhuo Xu et al.

Citation: *J. Appl. Phys.* **109**, 014108 (2011); doi: 10.1063/1.3530617

View online: <http://dx.doi.org/10.1063/1.3530617>

View Table of Contents: <http://jap.aip.org/resource/1/JAPIAU/v109/i1>

Published by the [AIP Publishing LLC](#).

---

### Additional information on *J. Appl. Phys.*

Journal Homepage: <http://jap.aip.org/>

Journal Information: [http://jap.aip.org/about/about\\_the\\_journal](http://jap.aip.org/about/about_the_journal)

Top downloads: [http://jap.aip.org/features/most\\_downloaded](http://jap.aip.org/features/most_downloaded)

Information for Authors: <http://jap.aip.org/authors>

### ADVERTISEMENT



**Running in Circles Looking  
for the Best Science Job?**

Search hundreds of exciting  
new jobs each month!

<http://careers.physicstoday.org/jobs>

physicstodayJOBS



# Electromechanical properties of $\text{Pb}(\text{In}_{1/2}\text{Nb}_{1/2})\text{O}_3\text{-Pb}(\text{Mg}_{1/3}\text{Nb}_{2/3})\text{O}_3\text{-PbTiO}_3$ single crystals

Fei Li,<sup>1,2</sup> Shujun Zhang,<sup>2,a)</sup> Dabin Lin,<sup>1,2</sup> Jun Luo,<sup>3</sup> Zhuo Xu,<sup>1</sup> Xiaoyong Wei,<sup>1</sup> and Thomas R. Shrout<sup>2</sup>

<sup>1</sup>Electronic Materials Research Laboratory, Key Laboratory of the Ministry of Education, Xi'an Jiaotong University, Xi'an 710049, People's Republic of China

<sup>2</sup>Materials Research Institute, Pennsylvania State University, University Park, Pennsylvania 16802, USA

<sup>3</sup>TRS technologies, Inc., 2820 East College Avenue, State College, Pennsylvania 16801, USA

(Received 29 September 2010; accepted 20 November 2010; published online 7 January 2011)

The  $\text{Pb}(\text{In}_{1/2}\text{Nb}_{1/2})\text{O}_3\text{-Pb}(\text{Mg}_{1/3}\text{Nb}_{2/3})\text{O}_3\text{-PbTiO}_3$  (PIN-PMN-PT) crystals were studied as function of phase and orientation. The properties, including the Curie temperature  $T_C$ , ferroelectric-ferroelectric phase transition temperature  $T_{R/O-T}$ , coercive field, and piezoelectric/dielectric responses, were systematically investigated with respect to the composition of PIN-PMN-PT crystals. The Curie temperature  $T_C$  was found to increase from 160 to 220 °C with ferroelectric-ferroelectric phase transition temperature  $T_{R-T}$  and  $T_{O-T}$  being in the range of 120–105 °C and 105–50 °C, respectively. The piezoelectric activity of PIN-PMN-PT crystals was analyzed by Rayleigh approach. The ultrahigh piezoelectric response for domain engineered [001] (1600–2200 pC/N) and [011] (830–1550 pC/N) crystals was believed to be mainly from the intrinsic contribution, whereas the enhanced level of piezoelectric and dielectric losses at the compositions around morphotropic phase boundaries (MPBs) was attributed to the phase boundaries motion.

© 2011 American Institute of Physics. [doi:10.1063/1.3530617]

## I. INTRODUCTION

The relaxor-PT based ternary  $\text{Pb}(\text{In}_{1/2}\text{Nb}_{1/2})\text{O}_3\text{-Pb}(\text{Mg}_{1/3}\text{Nb}_{2/3})\text{O}_3\text{-PbTiO}_3$  (PIN-PMN-PT) crystals, which can be readily grown by modified Bridgman method with large size (>70 mm in diameter), have been received considerable attention.<sup>1–7</sup> To date, investigations are mainly focused on the rhombohedral region of PIN-PMN-PT crystals. Compared to the binary  $\text{Pb}(\text{Mg}_{1/3}\text{Nb}_{2/3})\text{O}_3\text{-PbTiO}_3$  (PMN-PT) crystals, the rhombohedral PIN-PMN-PT crystals possess comparative piezoelectric coefficients ( $d_{33} > 1500$  pC/N) and electromechanical couplings ( $k_{33} > 0.90$ ), higher coercive field ( $E_C \sim 5$  kV/cm), and broadened temperature usage range ( $\sim 130$  °C). Those results demonstrated that the ternary PIN-PMN-PT crystals are promising candidates for electromechanical devices where high temperature usage and ac field stability are required. Furthermore, good properties were observed for orthorhombic and tetragonal PIN-PMN-PT crystals,<sup>8–11</sup> where high shear piezoelectric responses ( $d_{24}$ ) with improved temperature stability were obtained in orthorhombic crystals<sup>10,11</sup> while high electromechanical coupling factor  $k_{33}$  (>84%) and mechanical quality factor  $Q$  (>2000) were achieved in tetragonal crystals, with broadened temperature usage range (>200 °C).<sup>8</sup>

Thus, in order to better understand and illustrate the properties among the rhombohedral, orthorhombic, and tetragonal crystals, it is desirable to systematically study the PIN-PMN-PT crystals with various phases and compositions. In this study, the general characteristics, including dielectric and piezoelectric coefficients, Curie temperature  $T_C$ ,

ferroelectric-ferroelectric phase transition temperature  $T_{R/O-T}$ , and coercive field  $E_C$  of [001] and [011] poled PIN-PMN-PT crystals, were investigated as function of compositions with rhombohedral (R), orthorhombic (O), and tetragonal (T) phases. The approaches to distinguish the rhombohedral and orthorhombic/monoclinic phases for PIN-PMN-PT crystals were presented. The piezoelectric behaviors of [001] poled PIN-PMN-PT crystals were studied by Rayleigh analysis, in order to explore the origin of the ultrahigh piezoelectric response.

## II. EXPERIMENTS

The PIN-PMN-PT single crystals with nominal composition of  $x\text{PIN}-(1-x-y)\text{PMN}-y\text{PT}$ , where  $x > 0.25\text{--}0.35$ ,  $y > 0.30\text{--}0.32$ , were grown using the modified Bridgman technique.<sup>1</sup> The PT, PMN, and PIN contents were found to vary along the growth direction due to the different segregation coefficients of  $\text{Ti}^{4+}$ ,  $(\text{Mg}_{1/3}\text{Nb}_{2/3})^{4+}$ , and  $(\text{In}_{1/2}\text{Nb}_{1/2})^{4+}$  during the crystal growth process.<sup>5</sup> Thus, with the crystals' position away from the starting point of the crystal boule, the PT content increased, leading to the crystal structure and phase variations along the growth direction, from rhombohedral, via orthorhombic/monoclinic, to tetragonal phase. In this paper, the crystal samples were marked from 1 to 13 based on the positions. The crystals were oriented by real-time Laue technique. Vacuum sputtered gold was applied to the polished surface as the electrodes for all the samples. The [001] and [011] oriented rhombohedral and orthorhombic crystals were poled by applying 10 kV/cm dc electric field at room temperature, while for [001] oriented tetragonal crystals, the samples were poled at 250 °C by applying 2–3 kV/cm dc electric field, and field cooled to room tempera-

<sup>a)</sup>Electronic mail: soz1@psu.edu.

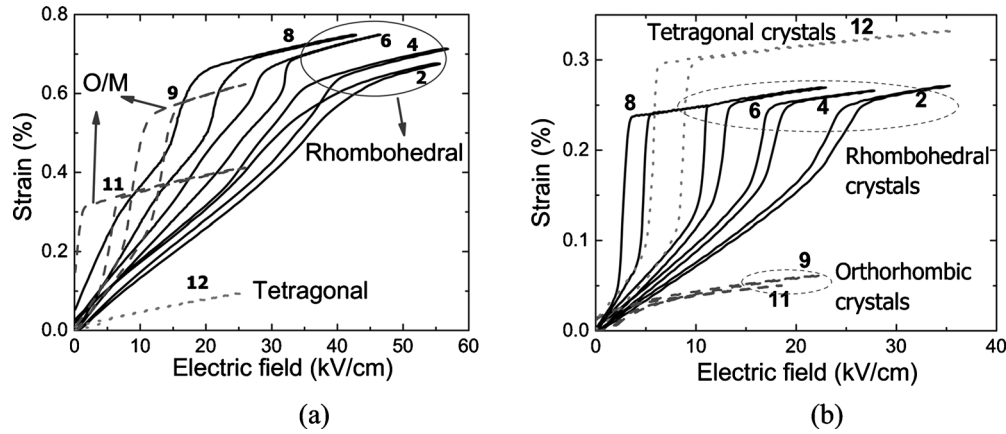


FIG. 1. Electric field vs strain behaviors for (a) [001] and (b) [011] poled PIN-PMN-PT crystals with various phases.

ture, to avoid the cracking. The piezoelectric coefficient  $d_{33}$  was measured by  $d_{33}$ -meter on plate samples. High field polarization and strain behaviors were determined using a modified Sawyer–Tower circuit and linear variable differential transducer (LVDT) driven by a lock-in amplifier (Stanford Research system, Mode SR830). The temperature dependence of the dielectric permittivity was determined using LCR meter (HP4284A), being connected to a computer controlled temperature chamber. For Rayleigh experiments, the [001] poled samples were cut to obtain longitudinal rods with dimensions of 2 mm × 2 mm × 8 mm, and the maximum amplitude of the applied electric field was selected to be 1 kV/cm, being smaller than the half of the coercive field for PIN-PMN-PT crystals (about 4–5 kV/cm).

### III. RESULTS AND DISCUSSION

#### A. Phase determination

##### 1. Strain-electric field behavior

The phase of relaxor-PT based crystals, such as PMN-PT and PZN-PT, can be determined to vary from rhombohedral, via monoclinic ( $M_C$ )/orthorhombic, to tetragonal phase with increasing PT content.<sup>12,13</sup> In this paper, the monoclinic  $M_C$  phases was recognized as pseudo-O phases from an viewpoint of application.<sup>11,14</sup>

By investigation of the PMN-PT crystals with various compositions,<sup>15</sup> we have showed a macroscopic method to distinguish the R, O, and T phases for PMN-PT crystals. Analogues to PMN-PT, the phases of PIN-PMN-PT crystals were determined by measuring the electric-field-induced-strain behaviors.

Figure 1(a) showed the electric-field-induced-strain for [001] poled PIN-PMN-PT crystals with various PT content. In rhombohedral phase, it can be seen that the electric field threshold for inducing tetragonal phase ( $E_T$ ) was decreased with increasing the PT content, with similar induced strain levels of  $S_{R-T}$  (from rhombohedral to tetragonal phase), being on the order of  $>0.65\%$ . As composition approaching R-O phase boundary, two phase transitions were observed (loop 6 and 8), i.e., R-M and M-T phase transitions, similar to PMN-PT crystals.<sup>15,16</sup>

For orthorhombic crystals, only one phase transition was observed, corresponding to orthorhombic-tetragonal phase transition. The electric-field-induced strain from orthorhombic to tetragonal phase ( $S_{O-T}$ ) was found to be less than 0.60% and drastically decreased with increasing the PT content. According to the analysis for PMN-PT crystals, this phenomenon can be attributed to the variation of the phase content in PIN-PMN-PT crystals.<sup>15</sup> The S-E characteristics for [001] poled PMN-PT and PIN-PMN-PT crystals were summarized in Table I.

The S-E loops of [011] poled PIN-PMN-PT crystals were shown in Fig. 1(b). The rhombohedral and orthorhombic crystals can be readily distinguished, where no phase transition occurs for orthorhombic crystals, due to the applied electric field being parallel to the spontaneous polar direction of the orthorhombic phase. In both [011] poled rhombohedral and tetragonal crystals, R-O or T-O phase transitions can be observed. The electric-field-induced-strain  $S_{R-O}$  was around 0.23% for rhombohedral crystals, while the strain  $S_{T-O}$  of tetragonal crystals was 0.31%, being larger than  $S_{R-O}$ . This is due to the angle between the polar direc-

TABLE I. Characteristics of C-vs-T and S-vs-E behaviors for [001] poled relaxor-PT crystals in rhombohedral (R) and orthorhombic (O) region.  $E_T$ , the required electric field for inducing tetragonal phase;  $strain_{R/O-T}$ , the electric-field-induced-strain from ground phase (R or O) to tetragonal phase. As demonstrated, the aim of this table is to provide a basis to distinguish the phase R and O.

	Phase	$T_{R/O-T}$ (°C)	$T_C$ (°C)	$E_T$ (kV/cm)	$Strain_{R/O-T}$ (%)	Characteristics of S-E behavior
PMN-PT	R	~95	<145	>30	~0.69	Two phase transition can be observed
	O/M	<90	145–170	<25	<0.6	Only one phase transition
PIN-PMN-PT	R	105–130	<185	>25	~0.67	Two phase transition can be observed
	O/M	<100	190–210	<20	<0.6	Only one phase transition

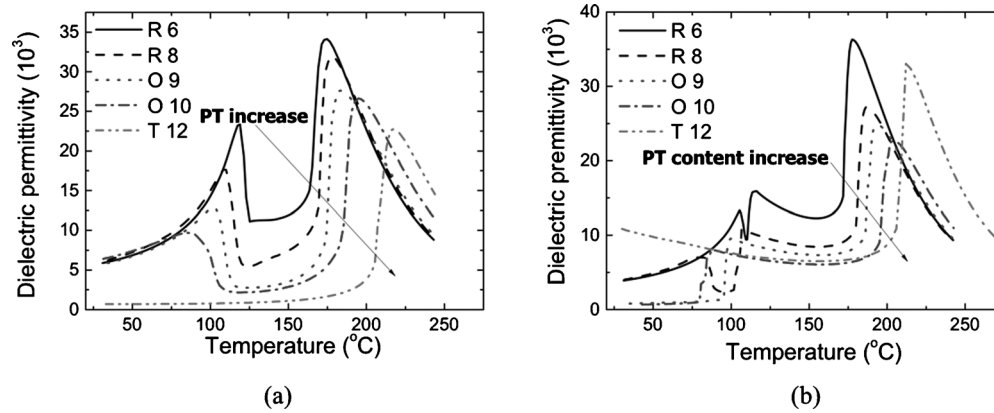


FIG. 2. Temperature dependent dielectric properties for (a) [001] and (b) [011] oriented PIN-PMN-PT crystals with various phases.

tions of rhombohedral and orthorhombic phase ( $\sim 35^\circ$ ) was smaller than that between the polar directions of tetragonal and orthorhombic phase ( $\sim 45^\circ$ ).

## 2. Dielectric behavior as function of temperature

Figure 2 and Table II showed the temperature dependent dielectric behaviors, in order to better understand the temperature induced phase transitions for PIN-PMN-PT crystals. For [001] and [011] poled rhombohedral crystals (samples 1–6), the Curie temperature  $T_C$  was found to increase from 160 to 175 °C with increasing the PT content, while the temperature  $T_{R-T}$  was changed slightly, being 123–119 °C. With further increasing the PT content, it can be seen that the phase transition temperature  $T_{R/O-T}$  decreased from 120 °C (sample 6) to 105 °C (sample 8), and two phase transitions can be observed for [011] poled crystals [Fig. 2(b)], corresponding to the rhombohedral-orthorhombic (R-O) and orthorhombic-tetragonal (O-T) phase transitions. For orthorhombic crystals (samples 9–11), the phase transition temperature  $T_{O-T}$  significantly decreased from 100 to 57 °C while the Curie temperature increased from 190 to 210 °C, being similar to the orthorhombic PMN-PT crystals. The te-

tragonal phase can be readily determined by dielectric permittivity-versus-temperature behaviors, due to no ferroelectric-ferroelectric phase transition occurs above room temperature, as can be confirmed in sample 12, where only one dielectric anomaly, corresponding to the  $T_C$ , was observed above 215 °C.

## B. Properties of [001] and [011] poled PIN-PMN-PT crystals

Table II summarized the room temperature properties for PIN-PMN-PT crystals, including the piezoelectric coefficient, dielectric permittivity, coercive field, Curie temperature, and ferroelectric-ferroelectric phase transition temperatures. The piezoelectric coefficient  $d_{33}$  and dielectric permittivity  $\epsilon_{33}/\epsilon_0$  of [001] and [011] poled rhombohedral crystals (samples 1–8) were generally increased as the composition approaches R-O phase boundary. For orthorhombic and tetragonal phase regions, the high piezoelectric coefficients and dielectric permittivities were observed for domain engineered crystals ([001] poled orthorhombic crystals and [011] poled tetragonal crystals), whereas those material con-

TABLE II. Properties of PIN-PMN-PT crystals with various compositions and phases. For [011] poled samples 7 and 8, both phase transition temperatures  $T_{R-O}$  and  $T_{O-T}$  are listed, where the  $T_{R-O}$  is in the brace.

Normalized position from cone	[001] poled crystals								[011] poled crystals							
	Phase (No.)	$T_{R/O-T}$ (°C)	$T_C$ (°C)	$E_C$ (kV/cm)	$d_{33}$ (pC/N)	$k_{33}$	$\epsilon_{33}/\epsilon_0$	Dielectric loss (%)	Phase (No.)	$T_{R/O-T}$ (°C)	$T_C$ (°C)	$E_C$ (kV/cm)	$d_{33}$ (pC/N)	$\epsilon_{33}/\epsilon_0$	Dielectric loss (%)	
0.08	R (1)	123	161	4.5	1400	0.89	3130	0.7	R (1)	...	...	...	...	...	...	
0.16	R (2)	122	162	4.3	1600	0.90	4700	0.6	R (2)	122	163	5.1	830	2800	0.4	
0.24	R (3)	122	168	4.3	1680	0.90	4600	0.8	R (3)	121	167	6.1	900	3050	0.3	
0.32	R (4)	121	168	4.8	1700	0.91	4700	0.7	R (4)	119	168	6.0	930	3420	0.3	
0.40	R (5)	121	171	5.0	1730	0.92	5500	0.8	R (5)	119	172	6.1	940	3000	0.4	
0.48	R (6)	119	174	4.6	2000+	0.92	5600	0.8	R (6)	117	175	6.4	1070	3660	0.5	
0.56	R (7)	112	179	4.2	2000+	0.92	5500	0.9	R (7)	{105} 115	178	7.2	1250	3900	0.6	
0.64	R (8)	105	183	4.3	2000+	0.93	5900	1.1	R (8)	{85} 106	185	6.5	1550	4000	1.0	
0.72	O (9)	90	193	4.5	2000+	0.93	6300	1.7	O (9)	100	193	5.0	220	900	0.6	
0.80	O (10)	78	199	4.1	1850	0.91	4200	1.3	O (10)	85	203	5.0	200	660	0.3	
0.88	O (11)	57	208	7.0	1910	0.91	4300	0.7	O (11)	60	207	5.0	170	630	0.4	
0.96	T (12)	None	217	6.4	450	0.85	800	0.3	T (12)	None	216	6.5	1000	8000	0.9	
1	T (13)	None	223	10	400	0.83	800	0.3	T (13)	None	222	10.5	900	7200	0.5	

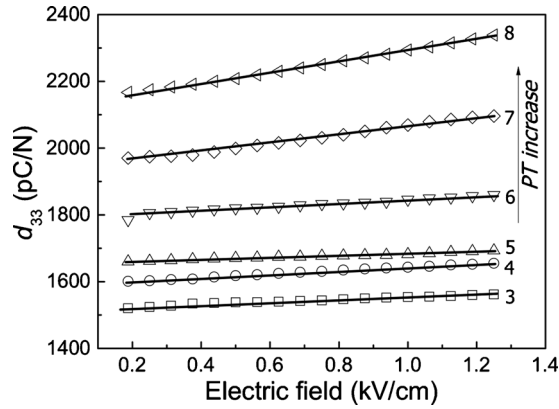


FIG. 3. The ac electric field dependent piezoelectric coefficient  $d_{33}$  for rhombohedral PIN-PMN-PT crystals with various compositions, measured at 1 Hz.

stants were relatively small for single domain crystals ([011] poled O crystals and [001] poled tetragonal crystals).

As shown in Table II, the variation in dielectric permittivity with respect to composition was similar to that of the piezoelectric coefficient. High level of dielectric losses were also observed for domain engineered crystals with the composition approaching morphotropic phase boundaries (MPBs) (up to 1.7%) while for the crystals with composition away from MPBs, the dielectric loss was relatively small, being around 0.7% and 0.5% for [001] and [011] poled domain engineered crystals, respectively. The details of the composition dependent piezoelectric/dielectric behaviors will be analyzed in Sec. III C.

In contrast to piezoelectric and dielectric activities, electromechanical coupling factor  $k_{33}$  was relatively stable with the composition, being on the order of 89%–93% for [001] poled crystals. As shown in Refs. 5 and 7, the electromechanical coupling factors were insensitive to their respective phase transition temperatures  $T_C$  and  $T_{RT}$ .

Coercive field is an important factor for high field applications, therefore, the variation in coercive field with respect to composition were measured. As listed in Table II, for rhombohedral phase, the [011] oriented PIN-PMN-PT crystals exhibited larger coercive fields, being on the order of 5–6 kV/cm, when compared to [001] oriented crystals (4–5 kV/cm), with maximum coercive field being 7.2 kV/cm, as the composition approaching to R-O phase boundary. For

[001] oriented orthorhombic crystals, the coercive field showed maximum value for the composition close to O-T phase boundary, being 7.0 kV/cm. In contrast to the [001] direction, the coercive of [011] oriented orthorhombic crystals were independent of the composition, being 5.0 kV/cm. In tetragonal region, the coercive fields of [001] and [011] oriented samples were increased from 6.5 to 10 kV/cm with increasing the PT content, higher than their R and O counterparts.

### C. Rayleigh analysis of the piezoelectric activity

The piezoelectric behaviors of [001] poled PIN-PMN-PT crystals were analyzed by Rayleigh approach.<sup>15,17</sup> Figure 3 showed the ac field dependent  $d_{33}(E_0)$  for the [001] poled rhombohedral crystals with various compositions, where a linear variation of  $d_{33}$  was observed. Based on Rayleigh analysis, the piezoelectric response can be expressed as the following equation:

$$d(E_0) = (d_{\text{init}} + \alpha E_0) \text{pC/N}, \quad (1)$$

where the coefficient  $d_{\text{init}}$  describes the reversible piezoelectric response, being mainly from the intrinsic (lattice) contribution for domain engineered crystals.<sup>15,18</sup> The coefficient  $\alpha$  is the irreversible Rayleigh parameter, resulting from the irreversible motion of the internal interfaces, and  $\alpha E_0$  represents the extrinsic contribution to the total piezoelectric response. For convenience,  $d_{\text{init}}$  is defined as a nonunit coefficient and the unit of  $\alpha$  is given as centimeter per kilovolt.

According to the fitting results, the Rayleigh parameters as a function of Curie temperature are given in Fig. 4, where the rhombohedral (R), orthorhombic (O), and tetragonal (T) regions were marked accordingly. It can be seen that the high piezoelectric response of PIN-PMN-PT crystals was mainly from the intrinsic contribution (>90%). The parameter  $d_{\text{init}}$  showed peak values at the compositions around MPBs. The maximum  $d_{\text{init}}$  was observed in rhombohedral crystals with compositions close to R-O phase boundary (sample 8), being on the order of 2200 pC/N. In domain engineered rhombohedral crystals, the high intrinsic piezoelectric activity was thought to be associated with the high shear piezoelectric coefficient of the corresponding single domain state, as expressed in the following equation:

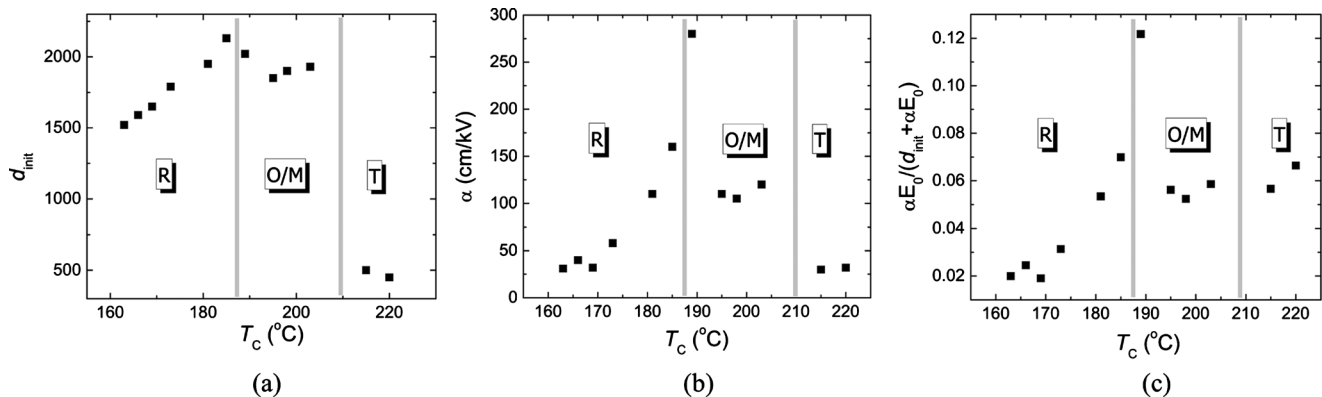


FIG. 4. Rayleigh parameters with respect to  $T_C$  (composition) for PIN-PMN-PT crystals, measured at 1 Hz.

$$d_{33}^{(001)} = (d_{15}^R + d_{31}^R) \cos \theta \sin^2 \theta + d_{22}^R \sin^3 \theta + d_{33}^R \cos^3 \theta, \quad (2)$$

where  $d_{33}^R$ ,  $d_{15}^R$ ,  $d_{31}^R$ , and  $d_{22}^R$  are single domain piezoelectric coefficients measured along principal crystallographic axes, and  $\theta$ , the angle between [111] and [001] axis, being about  $54^\circ$ . According to thermodynamic analysis,<sup>19</sup> the shear piezoelectric coefficient  $d_{15}^R$  in rhombohedral phase region will increase as the composition approaching R-O phase boundary, leading to the enhanced  $d_{\text{init}}$  with  $T_C$  increasing (PT content increasing). For orthorhombic crystals, the coefficient  $d_{\text{init}}$  was first decreased and then increased with the  $T_C$  increasing. As observed in PMN-PT crystals,<sup>15</sup> this phenomenon can be explained by the variation in shear coefficient and phase content in O region. Due to the applied field along the polar direction, low level of piezoelectric coefficient was observed in [001] poled tetragonal crystals.

Analogues to the piezoelectric response, the dielectric permittivity of [001] poled crystals was mainly contributed by the transverse dielectric permittivity  $\epsilon_{11}/\epsilon_0$ . As analyzed in Ref. 19, the variation in dielectric permittivity  $\epsilon_{11}/\epsilon_0$  with respect to composition was similar to that of shear piezoelectric coefficient  $d_{15}$ . Thus, the observed composition dependence of dielectric permittivity was similar to that of piezoelectric behavior.

By the same method, the dielectric/piezoelectric variation in [011] poled crystals versus composition can be explained. The increasing tendency of  $d_{33}$  and  $\epsilon_{33}/\epsilon_0$  in rhombohedral region can be attributed to the increase in  $\epsilon_{11}^R/\epsilon_0$  and  $d_{15}^R$  while for tetragonal crystals, the  $d_{33}$  and  $\epsilon_{33}/\epsilon_0$  values decreased as the composition move away from T-O phase boundary, which was associated with the decreasing in  $\epsilon_{11}^T/\epsilon_0$  and  $d_{15}^T$  (transverse dielectric and shear piezoelectric constant of tetragonal crystals).<sup>9</sup> As a note, the  $d_{33}$  and  $\epsilon_{33}/\epsilon_0$  values of O phase were quite small, due to [011] direction is the spontaneous polar direction of orthorhombic crystals.

The low levels of irreversible (extrinsic) piezoelectric contribution were observed for [001] poled PIN-PMN-PT crystals, where the ratio  $[\alpha E_0/(\alpha E_0 + d_{\text{init}})]$ , was generally less than 5% [as shown in Fig. 4(c)], due to the lack of domain wall motion in stable domain engineered configurations. For [001] poled tetragonal PIN-PMN-PT crystals, single domain state can be achieved,<sup>8</sup> thus domain wall motion was minimal and the ratio  $\alpha E_0/(\alpha E_0 + d_{\text{init}})$  was much smaller when compared to the polycrystalline ceramics (up to 40%).<sup>20</sup> The maximum ratio  $\alpha E_0/(\alpha E_0 + d_{\text{init}})$ , being on the order of 12%, was observed in orthorhombic region with the composition close to the R-O phase boundary. High ratio  $\alpha E_0/(\alpha E_0 + d_{\text{init}})$  corresponds to the high piezoelectric loss.<sup>17,20</sup> In addition, as listed in Table II, the maximum dielectric losses were observed for the crystals with compositions around MPBs. These high extrinsic piezoelectric responses and dielectric losses can be attributed to the enhanced phase boundaries motion at the composition around MPBs, as analyzed in Ref. 15.

## IV. CONCLUSION

The ferroelectric, dielectric, and piezoelectric properties of PIN-PMN-PT crystals with various compositions were measured along [001] and [011] directions. The variation in piezoelectric/dielectric activities, electric field induced strain, Curie temperature, phase transition temperature, and coercive field with respect to the composition and ferroelectric phase, can be used as a basis for the future investigations and applications, such as high temperature, high ac field, and/or high power transducer applications. Furthermore, the piezoelectric activities of PIN-PMN-PT crystals were analyzed by Rayleigh approach, where the obtained results indicated that the ultrahigh piezoelectric responses for domain engineered PIN-PMN-PT crystals mainly arise from intrinsic contribution.

## ACKNOWLEDGMENTS

The work was supported by NIH under Grant No. P41EB21820 and ONR. The authors from Xi'an Jiaotong University acknowledged the National Basic Research Program of China (973 Program) under Grant No. 2009CB623306, International Science & Technology Cooperation Program of China under Grant No. 2010DFR50480, and National Nature Science Foundation of China (Grant Nos. 10976022 and 50632030).

- <sup>1</sup>S. J. Zhang, J. Luo, W. Hackenberger, and T. R. Shrout, *J. Appl. Phys.* **104**, 064106 (2008).
- <sup>2</sup>J. Tian, P. D. Han, X. L. Huang, and H. X. Pan, *Appl. Phys. Lett.* **91**, 222903 (2007).
- <sup>3</sup>X. Liu, S. J. Zhang, J. Luo, T. R. Shrout, and W. Cao, *Appl. Phys. Lett.* **96**, 012907 (2010).
- <sup>4</sup>G. S. Xu, K. Chen, D. F. Yang, and J. B. Li, *Appl. Phys. Lett.* **90**, 032901 (2007).
- <sup>5</sup>S. J. Zhang, J. Luo, W. Hackenberger, N. P. Sherlock, R. J. Meyer, Jr., and T. R. Shrout, *J. Appl. Phys.* **105**, 104506 (2009).
- <sup>6</sup>L. Liu, X. Wu, X. Zhao, X. Feng, W. Jing, and H. S. Luo, *IEEE Trans. Ultrason. Ferroelectr. Freq. Control* **57**, 2154 (2010).
- <sup>7</sup>S. J. Zhang and T. R. Shrout, *IEEE Trans. Ultrason. Ferroelectr. Freq. Control* **57**, 2138 (2010).
- <sup>8</sup>F. Li, S. Zhang, Z. Xu, X. Wei, J. Luo, and T. R. Shrout, *J. Appl. Phys.* **107**, 054107 (2010).
- <sup>9</sup>F. Li, S. Zhang, Z. Xu, X. Wei, J. Luo, and T. R. Shrout, *J. Am. Ceram. Soc.* **93**, 2731 (2010).
- <sup>10</sup>F. Li, S. Zhang, Z. Xu, X. Wei, J. Luo, and T. R. Shrout, "Temperature independent shear piezoelectric response in relaxor-PbTiO<sub>3</sub> based crystals," *Appl. Phys. Lett.* **92** (to be published).
- <sup>11</sup>S. J. Zhang, F. Li, J. Luo, R. Xia, W. Hackenberger, and T. R. Shrout, *Appl. Phys. Lett.* **97**, 132903 (2010).
- <sup>12</sup>L. Bellaiche, A. Garcia, and D. Vanderbilt, *Phys. Rev. B* **64**, 060103 (2001).
- <sup>13</sup>B. Noheda, *Curr. Opin. Solid State Mater. Sci.* **6**, 27 (2002).
- <sup>14</sup>M. Davis, D. Damjanovic, and N. Setter, *Phys. Rev. B* **73**, 014115 (2006).
- <sup>15</sup>F. Li, S. Zhang, Z. Xu, X. Wei, J. Luo, and T. R. Shrout, *J. Appl. Phys.* **108**, 034106 (2010).
- <sup>16</sup>B. Noheda, Z. Zhong, D. E. Cox, G. Shirane, S. E. Park, and P. Rehrig, *Phys. Rev. B* **65**, 224101 (2002).
- <sup>17</sup>D. Damjanovic, *Phys. Rev. B* **55**, R649 (1997).
- <sup>18</sup>M. Davis, D. Damjanovic, and N. Setter, *J. Appl. Phys.* **100**, 084103 (2006).
- <sup>19</sup>M. Budimir, D. Damjanovic, and N. Setter, *J. Appl. Phys.* **94**, 6753 (2003).
- <sup>20</sup>D. Damjanovic and M. Demartin, *J. Phys.: Condens. Matter* **9**, 4943 (1997).